Journal of Solid State Chemistry **151,** 25–30 (2000)
doi:10.1006/jssc.1999.8608, available online at http://www.idealibrary.com on IDEAL®

Structural Studies of the Metal–Nonmetal Transition in Ru Pyrochlores

M. Field,* B. J. Kennedy,*,[1] and B. A. Hunter†

*School of Chemistry, The University of Sydney, Sydney, New South Wales 2006, Australia, and †Neutron Scattering Group, ANSTO, PMB 1, Menai, New South Wales 2234, Australia

Received August 25, 1999; in revised form November 19, 1999; accepted December 13, 1999

A combination of powder neutron and X-ray diffraction measurements were carried out in the pyrochlore type oxides $Bi_{2-x}Nd_xRu_2O_{7-y}$, $0 < x < 2$ in order to probe the structural changes that occur on going from the metallic oxides, $x < 0.75$, to the semiconducting oxides, $x > 0.75$. The relative small change in the cubic lattice parameter across the series (0.4%) provides clear evidence that the lengthening of the Ru–O bond lengths in the nonmetallic oxides and the contraction of the Ru–O–Ru angle is a result of the change in the electronic properties of the oxides. The studies also illustrate the importance of oxide vacancies for metallic conductivity in these oxides. Metallic conductivity occurs in oxides where the Ru–O–Ru angle is greater than 132.5° and there is a measurable oxygen nonstoichiometry.

INTRODUCTION

There has been a resurgence of interest in pyrochlore type oxides in recent times (1–8) due to the variety of physical properties these materials exhibit. A common theme of a number of these studies has been to probe the possible relationships between the oxygen vacancies in pyrochlores and their remarkable physical properties. Horowitz and co-workers (9) originally highlighted the structural importance of oxygen vacancies when they showed the presence of long-range oxygen-vacancy ordering in the pyrochlore $Pb_2Ru_2O_{6.5}$. Such oxygen-vacancy ordering has now been observed in a number of related pyrochlores (10–12). More recently the correlation between the structure, oxygen stoichiometry, and electronic properties has been well illustrated in the studies of Sleight and co-workers on the Tl–Ru–O pyrochlore (13–16). Stoichiometric $Tl_2Ru_2O_{7.00}$ is cubic ($Fd3m$) at room temperature and undergoes a first-order phase transition to an orthorhombic $Pnma$ structure below 150 K. This is in contrast to the nonstoichiometric oxide $Tl_2Ru_2O_{6.95}$, which is cubic down to 2 K. The physical properties of the ruthernates, including electrical conductivity, also depend on the precise stoichemetrystoichiometry. It is not uncommon for transition metal pyrochlores to exhibit a metal–nonmetal transition. A further example of the variable physical properties of the pyrochlores comes from studies of $Bi_2Ru_2O_{7-\delta}$ by Carbonio and co-workers (17) who extended our previous work (18) and showed that it is possible to control the oxygen stoichiometry, and hence the structure and conductivity of $Bi_2Ru_2O_{7-\delta}$, by altering the annealing conditions.

In parallel with these studies on unsubstituted pyrochlores, Kanno and co-workers have reported extensive studies of the physical properties of ruthenium oxides of the type $Bi_{2-x}Ln_xRu_2O_7$ and $Pb_{2-x}Ln_xRu_2O_{7-\delta}$, where Ln is Y, La, or a lanthanide (19–21). $Bi_2Ru_2O_{7-\delta}$ and $Pb_2Ru_2O_{6.5}$ are metallic whereas the lanthanide ruthernates are all semiconductors (22). Oxides of this type were first studied independently by Goodenougth (23) and Kemmler-Slack (24), and subsequent electronic structure calculations showed that the unoccupied Bi 6p states are close to the Fermi level and mix with the Ru 4d state via the framework oxygen (25, 26). In general, Kanno and co-workers used X-ray diffraction methods to probe structural changes in these oxides at the M–NM transition, although it is expected that the strong X-ray scattering power of Pb, Bi, and the lanthanides will limit the precision of such structural studies. Nevertheless, their studies show the same trends in the evolution of the structural behavior at the M–NM transition as found by Kennedy and Vogt (27) in their more precise powder neutron diffraction studies of unsubstituted $A_2Ru_2O_{7-\delta}$ oxides, where A = Y, Bi, La, or a lanthanide

The $A_2B_2O_6O'$ pyrochlore structure can be described as consisting of two interpenetrating networks, one of corner-sharing B_2O_6 octahedra and the other anticrystobalite A_2O' chains (28). The A_2O' sublattice is not essential for the stability of the structure and vacancies of both the A-type cations and O′ anions are common (28). Where the two types of oxygen atoms are not distinguished the formula is

[1] To whom correspondence should be addressed. E-mail: Bkennedy@chem.usyd.edu.au.

0022-4596/00 $35.00

written as $A_2B_2O_7$. The regular pyrochlore structure is cubic ($Fd\bar{3}m$) with the A-type cations at (1/2, 1/2, 1/2) and the B-type cations at (0,0,0). The two types of oxygen anions are at (x, 1/8, 1/8) for the O anions and (3/8, 3/8, 3/8) for the O′ atoms. Thus the structure is described by two variables, a and x. Previous studies have established that metallic conductivity in the ruthenium pyrochlores is related to the Ru–O bond lengths, which are longer in the nonmetallic (semiconducting) oxides, leading to a greater distortion of the RuO_6 octahedra and the Ru–O–Ru bond angle (27). The quantification of these structural features requires both a and x to be determined. Equally clear from published work is the correlation of the oxygen vacancies with metallic conductivity in those pyrochlores with polarizable A cations. Whangbo has argued that such vacancies serve to reduce the overlap repulsion associated with the 6s orbitals of the A cations (29, 30).

The aim of the current work was to precisely determine the structural changes that occur upon addition of neodymium to the metallic pyrochlore $Bi_2Ru_2O_7$. Neodymium was chosen in this work since it has an ionic size similar to bismuth, hence structural changes should be dominated by the electronic transition from semiconducting to metallic behavior.

EXPERIMENTAL

The required stoichiometric amounts of Bi_2O_3, (Ajax), Nd_2O_3 (Aldrich), and Ru powder (Aithaca Chemicals) to prepare ca. 15 g of sample were mixed with an acetone slurry and ground with a mortar and pestle until dry. The mixture was transferred to an alumina crucible and heated in a muffle furnace at 650°C for 17 h. The samples were then reground and reheated at 800°C for 72 h and then at 950°C for a further 24 h. After additional regrinding all the samples were then heated for 58 h at 1100°C, except $Bi_{1.25}Nd_{0.75}Ru_2O_7$, which was heated for 24 h at 1100°C. The two samples $Bi_{0.75}Nd_{1.25}Ru_2O_7$ and $Bi_{1.0}Nd_{1.0}Ru_2O_7$ were finally heated for an additional 30 h at 1200°C. A second series of samples, ca. 1.2 g each, with stoichiometries between $Bi_{1.0}Nd_{1.0}Ru_2O_7$ and $Bi_{1.25}Nd_{0.75}Ru_2O_7$ were also prepared and the final heat treatment for these samples was 100 h at 1200°C.

The X-ray diffraction data were collected on a Siemens D5000 diffractometer, using nonmonochromated Cu$K\alpha$ radiation. Data were collected in 0.02° steps between 10° and 120° with a counting time of 10 s per step. One milimeter divergence and antiscattering slits, 0.1-mm receiver, and 0.6-mm detector slits were used. The neutron powder diffraction data were collected using the High Resolution Powder Diffractometer (HRPD) at ANSTO's HIFAR facility (31). The HRPD currently has 24 detectors separated by 5°, and a germanium monochromator, take-off angle 120°, that was set to the (335) plane to obtain a wavelength of 1.49 Å. The beam size is 20×50 mm, and the flux at the sample is approximately 8×10^4 n/cm^2/s. The samples were housed in either 12 or 8 mm diameter vanadium cans and rotated during the measurements to minimise the effects of preferred orientation. The refinement of the structures used data collected in the 2θ range of 10–153° and a 2θ step size of 0.05°. Data were collected for 24 to 48 h. Temperature-dependent neutron diffraction data were collected in 0.1° steps at a wavelength of 1.667 Å on the medium resolution powder diffractometer at ANSTO's HIFAR facility (32).

The Rietveld refinement (33) of the combined neutron and X-ray data was undertaken with the PC version of the computer program LHPM (34). For the neutron diffraction profile the background was defined by a fourth-order polynomial in 2θ and was refined simultaneously with the profile parameters. A Voigt function was chosen to generate the line shape of diffraction peaks, in which the Gaussian component has widths given by the function (35): $(\mathrm{FWHM})^2 = U\tan^2\theta + V\tan\theta + W$, where U, V, and W are refinable parameters and the width of Lorentzian component was varied as $\eta\sec\theta$ to model particle size effects. For the X-ray diffraction profile the same background function was employed and a pseudo-Voigt function was chosen to generate the profile. Anisotropic displacement parameters were refined for all atoms. Refinements were continued until the parameter shifts in the last cycle were less than 10% of their associated esd's.

The lattice parameters of the various solid solutions were obtained from the powder X-ray diffraction data, collected for samples containing approximately 20 wt% tungsten as an internal standard, are listed in Table 1.

TABLE 1
Structural Parameters and Fit Criteria for Samples of $Bi_{2-x}Nd_xRu_2O_{7-y}$, from Combined Neutron and X-ray Data

Compound	a (Å)	x	N(Oxygen)	R_p	R_{wp}	"GOF"
$Bi_2Ru_2O_{7-\delta}$	10.2957(1)	0.3265(1)	6.907(9)	[a]	[a]	[a]
$Bi_{1.75}Nd_{0.25}Ru_2O_{7-\delta}$	10.3038(2)	0.3265(1)	6.907(9)	7.36	9.59	6.84
$Bi_{1.5}Nd_{0.5}Ru_2O_{7-\delta}$	10.3135(3)	0.3270(1)	6.938(9)	9.11	11.44	6.97
$Bi_{1.25}Nd_{0.75}Ru_2O_{7-\delta}$	10.3175(2)	0.3271(1)	6.955(12)	12.31	13.36	3.92
$Bi_{1.175}Nd_{0.825}Ru_2O_{7-\delta}$	10.3296(2)	0.3278(1)	6.996(13)	14.29	14.91	4.19
$Bi_{1.075}Nd_{0.925}Ru_2O_{7-\delta}$	10.3345(2)	0.3278(1)	6.977(14)	14.62	15.35	4.17
$Bi_{1.0}Nd_{1.0}Ru_2O_{7-\delta}$	10.3303(2)	0.3270(2)	6.963(16)	14.86	15.83	4.99
$Bi_{0.75}Nd_{1.25}Ru_2O_{7-\delta}$	10.3374(2)	0.3283(1)	6.978(12)	11.78	13.24	4.27
$Bi_{0.5}Nd_{1.5}Ru_2O_{7-\delta}$	10.3397(3)	0.3287(1)	6.982(10)	10.87	11.97	4.79
$Bi_{0.25}Nd_{1.75}Ru_2O_{7-\delta}$	10.3410(2)	0.3295(1)	6.988(9)	8.61	10.21	5.85
$Nd_2Ru_2O_{7-\delta}$	10.3433(3)	0.3302(2)	6.992(16)	7.27	9.88	7.58

Note. N is the stoichiometry of individual atoms, from site occupancy. The Rietveld refinements were done in the cubic space group $Fd3m$ (no. 227). The oxygen atoms are on sites 48f(x, 1/8, 1/8) and 8b(3/8, 3/8, 3/8). The numbers in parentheses are the estimated standard deviations in the last significant digit.

[a] Values from Ref. (18).

RESULTS AND DISCUSSION

The strategy used to obtain accurate structural parameters for the series of oxides $Bi_{2-x}Nd_xRu_2O_{7-\delta}$ was as follows. First, the lattice parameter of the oxides were determined used a conventional (Cu$K\alpha$) powder diffractometer, where tungsten ($a = 3.1650$ Å) was added as an internal standard. Next, a second X-ray diffraction data set was collected for each sample and this was jointly analyzed with the appropriate powder neutron diffraction data. In the joint analysis the lattice parameter was constrained to the value obtained from the analysis of the X-ray diffraction pattern for the *W* containing sample and the diffractometer zero points and neutron wavelength allowed to vary in the Rietveld refinements.

Figure 1 demonstrates that the replacement of the bismuth with neodymium in $Bi_{2-x}Nd_xRu_2O_{7-\delta}$ results in an increase in the lattice parameter, *a*, even though neodymium has a smaller ionic radii than bismuth (36). The lattice parameter–composition curve does not obey Vegard's law, as first noted by Cox *et al.* (22) in their study of $Bi_{2-x}Gd_xRu_2O_{7-\delta}$ and later confirmed by Kanno and co-workers for the series of $Bi_{2-x}Ln_xRu_2O_{7-\delta}$ oxides (19, 21). There is a discontinuity in the lattice parameters near $x = 0.875$, as shown by the doted line in Fig. 1, corresponding to the transition between the metallic and nonmetallic oxides. This is in good agreement with the study of Kanno and co-workers (21). Whangbo *et al.* suggested that increasing the effective ionic radii of the *A*-site cation will result in greater repulsion of the oxygen atoms and therefore larger Ru–O–Ru bond angles so to stabilize the metallic state (29, 30). If this repulsion was the only structural influence on conductivity then it is envisaged that there should be a continuous change between the metallic and nonmetallic states. That this is not observed indicates that other effects are also important and that a more sophisticated model is necessary to describe the changes in conductivity with structure. In an attempt to better define the discontinuity in the lattice parameter, a second series of samples were prepared. The lattice parameters for these samples, shown as triangles in Fig. 1, are systematically higher than those obtained in the first series of compounds and illustrate the sensitivity of the structures of these oxides to the precise preparative conditions. Further studies are planned in order to identify the factors important in these changes.

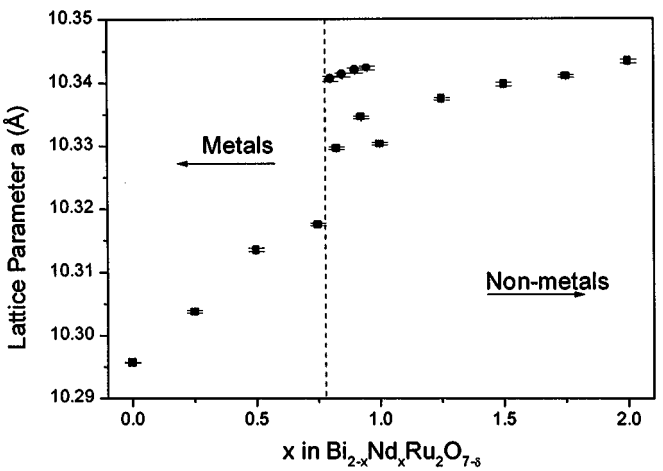

FIG. 1. Compositional dependence of the room temperature lattice parameters for $Bi_{2-x}Nd_xRu_2O_{7-\delta}$. The triangles correspond to values for a second series of compounds heated for a longer period of time. The vertical line separates the metallic Bi-rich compounds from the nonmetallic Nd-rich compounds.

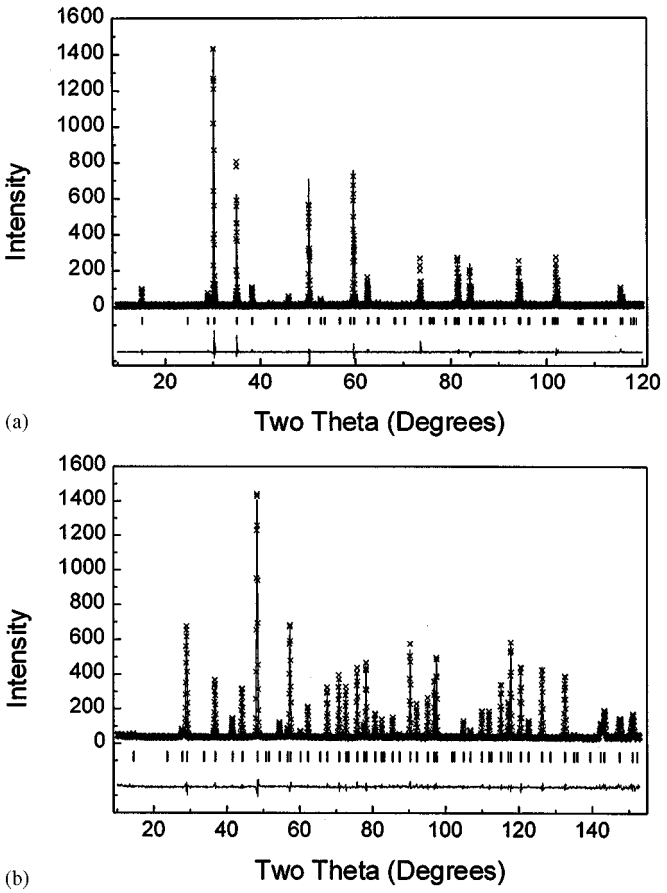

FIG. 2. Observed, calculated, and difference diffraction patterns for the (a) neutron and (b) X-ray data for $Bi_{2-x}Nd_xRu_2O_{7-\delta}$ at room temperature ($x = 0.5$). The solid line represents the calculated profile, and the crosses represent the observed intensities. The short vertical markers below the profiles mark the positions of the Bragg reflections.

The results of the structural refinements using a combination of powder neutron and X-ray diffraction data are summarized in Table 1, together with the criteria of fit. Representative examples of neutron and X-ray diffraction refinement profiles are given in Fig. 2. The single variable positional parameter, *x* of the oxygen atoms, shows a systematic reduction upon replacement of the bismuth with

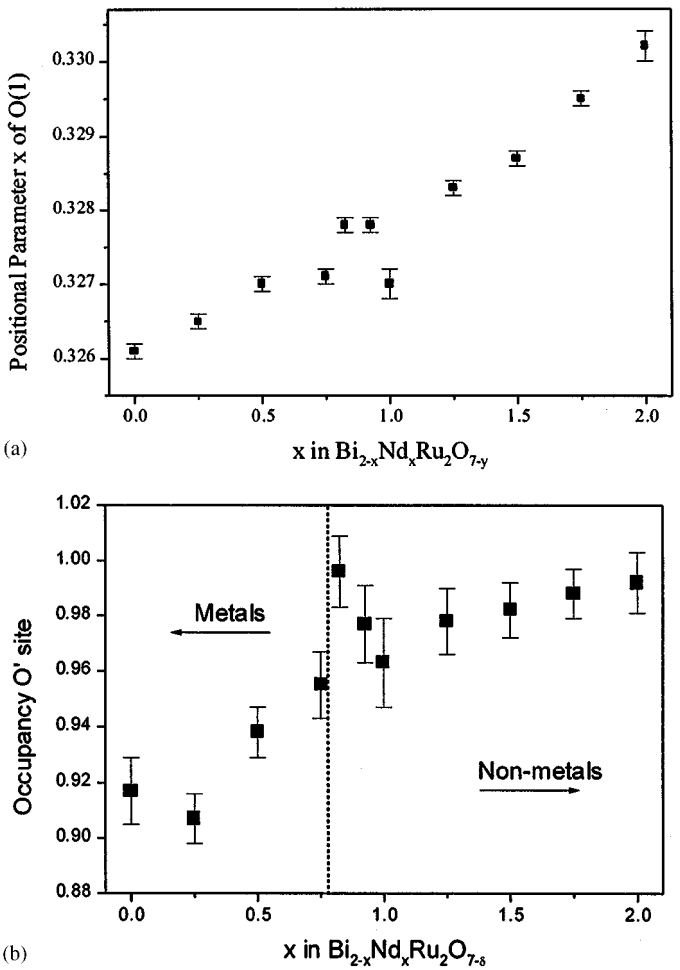

FIG. 3. Composition dependence of (a) the oxygen positional parameter and (b) the relative occupancy of the O 8*b* site for $Bi_{2-x}Nd_xRu_2O_{7-\delta}$.

neodymium, as the RuO_6 octahedra become more distorted (Fig. 3).

The structural refinements indicated that a number of the oxides had vacancies on the O′ site, and the variation of this with composition is illustrated in Fig. 3. Samples with $x > 0.75$ appear to have a near fully occupied O′ site since in all cases the refined site occupancy is within two standard deviations of that of a fully occupied site. Samples with $x \leq 0.75$ have a significant number of vacancies at the O′ site. As described in more detail below, these samples are the metallic oxides.

The sample with $x = 1$, $Bi_{1.0}Nd_{1.0}Ru_2O_7$ had anomalous values for the major structural parameters. This is possibly due to either local ordering of bismuth and neodymium or to more subtle effects arising from the annealing process. There is no evidence for any long range ordering that would lower the symmetry and result in additional reflections in the diffraction patterns.

The bond distances, bond angles, and bond-valence values from the refined structures are listed in Table 2. The values listed for $Nd_2Ru_2O_7$ were obtained in the present work by a combined analysis of X-ray diffraction and the previously reported neutron diffraction data (27).

The Ru–O bond distance increases as the neodymium content is increased, although examination of the results presented in Table 2 suggests that there is a discontinuity near $x \approx 0.75$, at the *M*–*NM* transition. This is illustrated in the dependence of the Ru–O distance on the lattice parameter, Fig. 3, where in the nonmetallic oxides the Ru–O distance increases more rapidly with lattice size than in the case of the metallic oxides. Kanno and co-workers have found (21) that the room temperatures resistivity of the oxides $Bi_{2-x}Nd_xRu_2O_{7-\delta}$ increase with increasing x and that a change from metallic to semiconducting behavior is observed at $x \approx 1.2$, i.e., for $Bi_{0.8}Nd_{1.2}Ru_2O_{7-\delta}$.

Replacing Bi with the smaller Nd in the oxides results in a decrease in the average Bi(Nd)–O bond distance. The contraction in the Bi(Nd)–O distance mirrors the expansion in the Ru–O distance in the nonmetallic oxides as illustrated in Fig. 3. In contrast, in the metallic oxides the Bi(Nd)–O distance is almost independent of the lattice parameter. The Ru–O–Ru angle shows a similar variation with lattice parameter to the Bi(Nd)–O bond distance, that is, it is almost constant in the metallic oxides and shows a systematic decrease as the lattice parameter increases in the nonmetallic oxides.

The behavior of both the bond distances and the Ru–O–Ru angle in the nonmetallic oxides mimics that seen in the series of nonconducting $La_2Sn_2O_7$ oxides (7). This suggests that the variation of the lattice parameters in the nonmetallic oxides is related to the changes in the RuO_6 geometry. The geometrical arguments, presented by Whangbo, that increasing the effective ionic radii of the *A*-type cation will increase the Ru–O–Ru bond angle and decrease the Ru–O bond distances is clearly correct for the nonmetallic oxides (29, 30). In this study, the Ru–O–Ru angle increases with increasing size of the weighted average ionic radii as expected, and there is a good linear relationship between the bond angle and the ionic radii, consistent with that found for the unsubstituted $A_2Ru_2O_7$ compounds (27). This indicates that the repulsion of the O anions by the *A*-site cations is critical in determining both the Ru–O–Ru angle and the Ru–O distance.

A second striking feature, seen in Fig. 4, is that the metallic oxides (bismuth rich) have Ru–O–Ru bond angles above 132.5°, while the nonmetallic neodymium-rich samples have lower bond angles. The width of the t_{2g}-block bands in $A_2Ru_2O_7$ is found to increase with increasing Ru–O–Ru bond angle due to a π-type orbital interaction through the Ru–O–Ru bridges (29). The present findings complement those of Sleight *et al.* (13, 14) who found that altering the oxygen stoichiometry in $Tl_2Ru_2O_7$ resulted in

TABLE 2
Selected Bond Distances, Bond Angles, and Bond Valence from the Structures Refined in This Work for the Series $Bi_{2-x}Nd_xRu_2O_{7-y}$

Stoichiometry	Ru–O (Å)	Bi(Nd)–O (Å)	Bi(Nd)–O′ (Å)	Ru–O–Ru angle (°)	Bi(Nd)–O–Bi(Nd) (°)	Bond valence Ru	Bond valence Nd/Bi	Conductivity Ref. (19)
$Bi_2Ru_2O_{7-\delta}$ [18]	1.984	2.576	2.229	133.1				M
$Bi_{1.75}Nd_{0.25}Ru_2O_{7-\delta}$	1.9849(3)	2.5519(5)	2.2308	133.18(4)	91.08(2)	3.99	3.13	M
$Bi_{1.5}Nd_{0.5}Ru_2O_{7-\delta}$	1.9887(3)	2.5508(5)	2.2329	132.92(4)	91.24(2)	3.95	3.15	M
$Bi_{1.25}Nd_{0.75}Ru_2O_{7-\delta}$	1.9899(4)	2.5511(8)	2.2338	132.86(6)	91.28(4)	3.94	3.18	M
$Bi_{1.175}Nd_{0.825}Ru_2O_{7-\delta}$	1.9950(5)	2.5494(8)	2.2364	132.50(6)	91.50(4)	3.88	3.18	M
$Bi_{1.075}Nd_{0.925}Ru_2O_{7-\delta}$	1.9957(5)	2.5506(9)	2.2374	132.51(7)	91.49(4)	3.88	3.18	M
$Bi_{1.0}Nd_{1.0}Ru_2O_{7-\delta}$	1.9920(6)	2.5550(11)	2.2366	132.92(8)	91.24(5)	3.92	3.18	M
$Bi_{0.75}Nd_{1.25}Ru_2O_{7-\delta}$	1.9991(4)	2.5468(8)	2.2381	132.16(6)	91.70(3)	3.84	3.23	NM
$Bi_{0.5}Nd_{1.5}Ru_2O_{7-\delta}$	2.0009(4)	2.5429(7)	2.2386	131.98(5)	91.81(3)	3.82	3.25	NM

an increase in the Ru–O–Ru bond angle in the metallic oxides.

The above results clearly demonstrate a smooth variation in the geometry of the *A*–O and hence the Ru–O contacts as Nd replaces Bi. Yet the variation in the lattice parameter is far from smooth at the *M–NM* transition and the Ru–O contacts in the metallic oxides are invariably only weakly dependent on the lattice parameter. We can reconcile these conflicting observations by recalling that the geometry of the *A*-type cation is a highly compressed $AO_6O'_2$ scalehedron (28). The Bi bond valence is dominated by the Bi–O′ bond (37, 38), hence a change in the Bi(Nd)–O′ bonding influences the *M–NM* transition. It is possible that these changes are due to the participation of the $6s^2$ lone pair of Bi^{3+} in the bonding. The sterochemical activity of these electrons in a BiO_8 environment is well documented (39) and acts to increase the effective size of the ion, provided there is no long range ordering of their displacement. In $Pb_2Ru_2O_{6.5}$ the analogous Pb $6s^2$ electrons are influential in the observed oxygen-vacancy ordering (9).

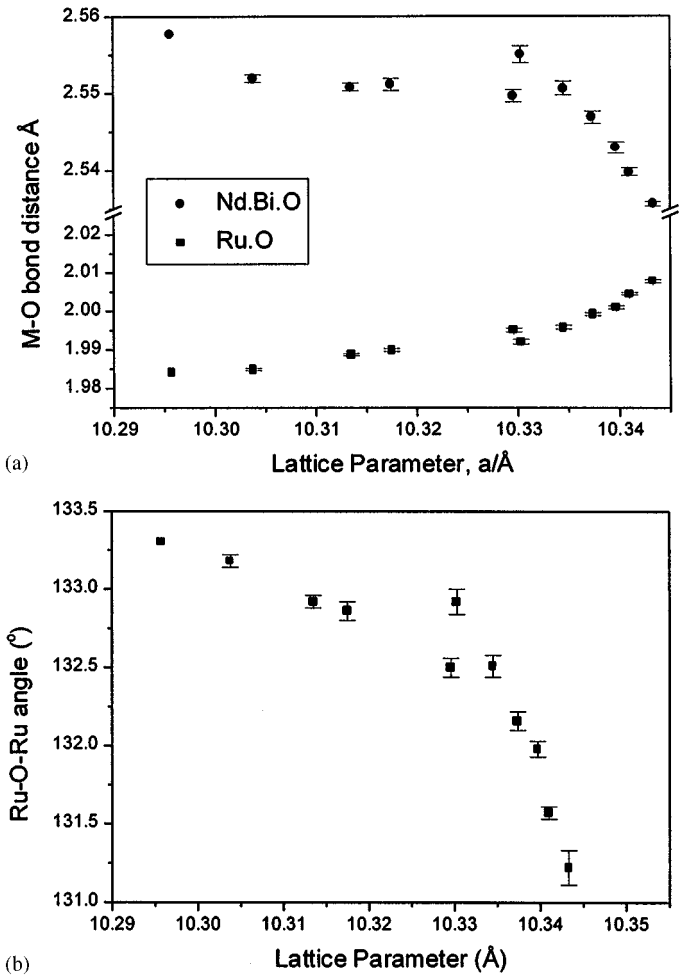

FIG. 4. Lattice parameter dependence of the (a) Ru–O and Bi/Nd–O distances and (b) the Ru–O–Ru angles for $Bi_{2-x}Nd_xRu_2O_{7-\delta}$ at room temperature.

At this stage it is appropriate to compare the present structural results with those presented by Kanno and coworkers (21). The estimated standard deviations (esd) of the structural parameters reported by Kanno are considerably larger than those found in this study, due to their sole use of powder X-ray diffraction data. In all cases, the values found in the present work fall within the range of 2 esd of the values reported by Kanno. The large magnitude of the esd in Kanno's work masks a systematic difference between the two studies. The oxygen positional parameter reported by Kanno (0.321(6)) (21) is significantly lower than that found either by Facer *et al.* (18) for $Bi_2Ru_2O_{6.9}$ (0.3265(1)) or Carbonio *et al.* (17) for $Bi_2Ru_2O_{6.8}$ (0.3271(3)). Here the final figure in parentheses is the reported esd. We have refined the structures of the present series of compounds using X-ray diffraction data alone and we have failed to confirm the low value of x reported by Kanno *et al.* It is possible that the different synthesis conditions employed by Kanno *et al.* (sealed Pt tubes) is the origin of this difference and we suggest that in their sample $y \approx 0$.

In addition to our detailed studies of the room temperature studies, we undertook variable temperature structural

studies (20–300 K) of two Bi-rich compounds $Bi_{2-x}Nd_x Ru_2O_{7-\delta}$ $x = 0.25$ and 0.5. As indicated above, both these compounds are metallic and have oxygen vacancies on the O′ site. For both compounds the low temperature diffraction data showed no evidence of a structural transition between 20 and 300 K. There was no apparent superstructure, peak splitting, or peak broadening at low temperatures. The plot of the lattice parameters with temperature shows no indication of any structural transition.

Low temperature neutron diffraction studies have revealed evidence for short-range magnetic ordering in the pyrochlores $Y_2Mn_2O_7$ and $Tb_2Mo_2O_7$ (40). Careful comparison of the diffraction patterns collected at room temperature and at 20 K did not reveal any significant differences indicative of a low temperature magnetic ordered state. Recent magnetic studies of both $Y_2Ru_2O_7$ and $Lu_2Ru_2O_7$ show these transform to a spin glass state at low temperatures (8).

In conclusion, we have clearly demonstrated the importance of oxygen vacancies in the A_2O' network in influencing the electronic properties of doped bismuth ruthernates. Based on this work and the previous studies there are four requirements for metallic conductivity in the ruthenium pyrochlores, namely: (I) The *A*-site cation needs to contain a polarizable cation, such as Bi^{3+}, Pb^{2+}, or Tl^{+}, (II) the Ru–O bond distance needs to be less than 2.00 Å, (III) the Ru–O–Ru bond angle needs to be greater than 132.5°, and (IV) there needs to be measurable vacancies in the oxygen sublattice. The sensitivity of these materials to small changes in preparative conditions is well illustrated for $Bi_2Ru_2O_{7-\delta}$, and this explains some of the discrepancies in the reported structural and physical properties of these materials. It remains to be determined if it is possible to exploit this sensitivity to tailor the *M–NM* transition by simply changing the oxygen stoichiometry in a manner similar to that found for $Tl_2Ru_2O_{7-\delta}$.

ACKNOWLEDGMENTS

This work has been partially supported by the Australian Institute of Nuclear Science and Engineering and the Australian Research Council.

REFERENCES

1. G. Gokagac and B. J. Kennedy, *J. Electroanal. Chem.* **368,** 235 (1994).
2. J. L. Fourquet, H. Duroy, and Ph. Lacorre, *J. Solid State Chem.* **114,** 575 (1995).
3. A. T. Ashcroft, A. K. Cheetham, J. S. Foord, M. L. H. Green, C. P. Grey, A. J. Murrell, and P. D. F. Vernon, *Nature* **344,** 319 (1990).
4. T. R. Felthouse, P. B. Fraundorf, R.M. Friedman, and C. L. Schosser, *J. Catal.* **127,** 421 (1991).
5. Y. Shimakawa, Y. Kubo, and T. Manako, *Nature* **379,** 53 (1996).
6. A. W. Sleight and R. Wang, R. *Mater. Res. Bull.* **33,** 2005 (1998).
7. B. J. Kennedy, B. A. Hunter, and C. J. Howard, *J. Solid State Chem.* **126,** 261 (1997).
8. N. Taira, M. Wakeshima, and Y. Hinatsu, *J. Solid State Chem.* **144,** 216 (1999).
9. R. A. Beyerlein, H. S. Horowitz, J. M. Longo, M. E. Leonowicz, J. D. Jorgenson, and F. J. Rotella, *J. Solid State Chem.* **51,** 253 (1984).
10. J. A. Alonso, C. Cascales, I. Rasines, and J. Pannetier, *Acta Crystallogr. Sect. C* **45,** 3 (1989).
11. B. J. Kennedy, *J. Solid State Chem.* **123,** 14 (1996).
12. Ismunandar, B. J. Kennedy, and B. A. Hunter, *J. Solid State Chem.* **130,** 81 (1996).
13. T. Takeda, M. Nagata, H. Kobayashi, R. Kanno, Y. Kawamoto, M. Takano, T. Kamiyama, F. Izumi, and A. W. Sleight, *J. Solid State Chem.* **140,** 182 (1998).
14. T. Takeda, R. Kanno, Y. Kawamoto, M. Takano, F. Izumi, A. W. Sleight, and A. W. Hewat, *J. Mater Chem* **9,** 215 (1999).
15. R. Kanno, J. Huang, and A.W. Sleight, *in* "Proceedings of the Fifth International Symposium on Advanced Nuclear Energy Research," **P-127,** 1994.
16. H. S. Jarrett, A. W. Sleight, J. F. Weiher, J. L. Gillson, C. G. Frederick, G. A. Jones, R. S. Swingle, D. Swatzfager, J. E. Gulley, and P. C. Hoell, *in* "Valence Instabilities and Related Narrow Band Phenomena (R. D. Parks, Ed.), p. 545. Plenum, New York, 1977.
17. R. E. Carbonio, J. A. Alonso, and J. L. Martinez, *J. Phys. Condens. Matter* **11,** 361 (1999).
18. G. Facer, M. M. Elcombe, and B. J. Kennedy, *Aust. J. Chem.* **46,** 1897 (1993).
19. R. Kanno, Y. Takeda, T. Yamamoto, Y. Kawamoto, and O. Yamamoto, *J. Solid State Chem.* **102,** 106 (1993).
20. H. Kobayashi, R. Kanno, Y. Kawamoto, T. Kamiyama, F. Izumi, and A. W. Sleight, *J. Solid State Chem.* **114,** 15 (1995).
21. T. Yamamoto, R. Kanno, Y. Takeda, O. Yamamoto, Y. Kawamoto, and M. Takano, *J. Solid State Chem.* **109,** 372 (1994).
22. P. A. Cox, J. B. Goodenougth, P. J. Tavener, D. Telles, and R. G. Edgell, *J. Solid State Chem.* **62,** 360 (1986).
23. J. B. Goodenougth, A. Hamnett, and D. Telles, *in* "Localization and Metal–Insulator Transition" (H. Fritzsche and D. Adler, Eds.). Plenum, New York, 1985.
24. A. Ehmann and S. Kemmler-Sack, *Mater. Res. Bull.* **20,** 437 (1985).
25. P. F. Carcia, A. Ferreti, and A. Suna, *J. Appl. Phys.* **53,** 5282 (1982).
26. W. Y. Hsu, R. V. Kasowski, T. Miller, and T. C. Chiang, *Appl. Phys. Lett.* **52,** 7 (1988).
27 B. J. Kennedy and T. Vogt, *J. Solid State Chem.* **126,** 261 (1996).
28. M. A. Subramanian, G. Aravamudan, and G. V. Subba Rao, *Prog. Solid State Chem.* **15,** 55 (1983).
29. M. H. Whangbo, K. S. Lee, and D. K. Seo, *J. Solid State Chem.* **131,** 405 (1997).
30. M. H. Whangbo, B.J. Kennedy, and H. J. Koo, *J. Solid State Chem.* **136,** 269 (1998).
31. C. J. Howard, C. J. Ball, R. L. Davis, and M. M. Elcombe, *Aust. J. Phys.* **36,** 507 (1983).
32. S. J. Kennedy, *Adv. X-Ray Anal.* **38,** 35 (1995).
33. H. M. Rietveld, *J. Appl. Cryst.* **2,** 65 (1969).
34. R. J. Hill and C. J. Howard, "Australian Atomic Energy Commission Report No. M112," 1986.
35. G. Caglioti, A. Paoletti, and F.P. Ricci, *Nucl. Instrum.* **2,** 223 (1958).
36. R. D. Shannon, *Acta Crystallogr. Sect. A* **32,** 751 (1976).
37. I. D. Brown and D. Altermatt, *Acta Crystallogr. Sect. B* **41,** 244 (1985).
38. I. D. Brown, *Acta Crystallogr. Sect. B* **48,** 553 (1992).
39. Ismunandar, Ph.D. thesis, The University of Sydney, 1998.
40. J. N. Reimers, J. E. Greedan, and M. Sato, *J. Solid State Chem.* **72,** 390 (1988).